25th ABCM International Congress of Mechanical Engineering
October 20-25, 2019, Uberlândia, MG, Brazil

COB-2019-0827
IMPROVING THE POLYNOMIAL REPRODUCIBILITY FOR THE PARTITION OF UNITY IN THE C^k-GENERALIZED FEM

Mateus Afonso Garbuio
Diego Amadeu F. Torres
Department of Mechanical Engineering - Federal University of Technology of Paraná - UTFPR - Londrina
mateus.garbuio@gmail.com, diego.amadeu@gmail.com

Abstract. *In this work, an improvement on the polynomial reproducibility of the C^k-Generalized Finite Element Method (C^k-GFEM) is achieved by assigning a polynomial basis to its Partitions of Unity (PoU) via Moving Least Squares (MLS). The construction of the weighting functions is similar to the conventional C^k-GFEM, while employing a polynomial basis alternatively to the Shepard functions when building the PoU. A study considering the one-dimensional elastostatic problem is presented, producing approximations by the present method and conventional FEM with Lagrangian shape functions for comparison. Extrinsic enrichment, as in the conventional GFEM, is also used. Numerical results in the form of relative errors in the L^2 norms and the convergence rates are presented. The results suggest that the intrinsic enrichment via MLS improves the approximation in the context of C^k-GFEM without the need of an extrinsic enrichment, while being able to better approximate regular fields if compared to the conventional Lagrangian shape functions, and keeping the arbitrariness of the parameters h, p and k as in original C^k-GFEM.*

Keywords: *Moving Least Squares Method, Intrinsic Enrichment, Extrinsic Enrichment, Smoothness, Generalized Finite Element Method*

1. INTRODUCTION

Mesh-free techniques as the Element-Free Galerkin Method (EFGM) (Belytschko *et al.*, 1994) and hp-Clouds Method (Duarte and Oden, 1996), mesh-based enriched methodologies using the Partition of Unity (PoU) concept, such as the Generalized / eXtended Finite Element Method (GFEM / XFEM) (Moës *et al.*, 1999; Duarte *et al.*, 2000; Belytschko *et al.*, 2001), unconventional approaches as the C^k-Generalized Finite Element Method (C^k-GFEM) (Duarte *et al.*, 2006) and the Smoothed FEM (Liu *et al.*, 2007), as well the Isogeometric Analysis (Cottrell *et al.*, 2007), have become alternatives to the conventional FEM analysis as the solution of some challenging problems cannot be succeed by approximations using simple piecewise polynomial shape functions.

In particular, the C^k-GFEM has shown interesting capabilities when applied to solid mechanics (de Barcellos *et al.*, 2009; Mendonça *et al.*, 2013; Torres *et al.*, 2015), while sharing similar features of FEM in terms of computational costs and inheriting the robustness of GFEM / XFEM. As a mesh-based method, the C^k-GFEM allows the conventional GFEM / XFEM, which generally uses C^0 linear shape functions[1] as PoU, to recover the smoothness commonly obtained in mesh-free methods based on the Moving Least Squares (MLS) (Liu, 2003), as the EFGM, and grants an arbitrariness on the k-continuity parameter choice.

On the effects caused by the higher regularity, Surana *et al.* (2001) firstly brought the smoothness as a refinement parameter of discretizations, but the so-called k-refinement has attracted much attention after the Isogeometric method (Cottrell *et al.*, 2007), from which a significant increase in accuracy was obtained for structural vibration problems, for instance, as a consequence of the continuity achieved by non-uniform rational b-splines approximation functions.

Even exhibiting versatile features for a mesh-based methodology, the C^k-GFEM suffers from low polynomial reproducibility, demanding extrinsic polynomial $p = 1$ enrichment in order to have linear consistency as the conventional C^0-GFEM / XFEM already reaches without enrichment. Differently, the PoU functions in C^k-GFEM are rational as they are constructed by MLS with a constant basis, recognized as Shepard functions (Schweitzer, 2008). In this way, the C^k-GFEM can demand more degrees of freedom than the C^0-GFEM for a given level of error (Torres *et al.*, 2015).

Originally, the C^k-GFEM of Duarte *et al.* (2006) leads to a C^∞-smoothness in case of meshes with only convex clouds, and this maximum continuity may stiff the discretization due to its strong oscillatory character. Still, it was shown by Malagù *et al.* (2014) that the b-spline approximation with C^1-continuity exceeds the performance of the C^∞-GFEM. However, in case of conventional b-splines, the k-refinement cannot be performed without increasing the p degree and

[1] In two-dimensional models, for instance, the tent functions for triangles or the Lagrangian linear functions for quadrilaterals are used as PoU.

enlarging the support of the functions, impacting the sparsity of the stiffness matrix.

In this work, the procedure presented by de Barcellos *et al.* (2009) is used along with the MLS (Lancaster and Salkauskas, 1981) in order to obtain PoU functions with an intrinsically $p = 1$ polynomial reproducibility, which can be done by enlarging the support of such functions. The resulting PoU functions can be further extrinsically enriched as in conventional GFEM / XFEM. Herein, the performance of such methodology is investigated in one-dimensional elastostatic problems.

The procedure keeps the k, p and h-refinements completely free, as in the original C^k-GFEM, in which the continuity k relies only on the choice of appropriate edge functions, which can assume polynomial or exponential forms (de Barcellos *et al.*, 2009). This k-continuity assignment itself does not require an enlargement of the function's support nor demand increment on the final p-degree of the functions. The p-degree of an approximation, in turn, is defined in two stages: firstly, a $p = 1$ degree of consistency for the PoU is obtained via intrinsic enrichment through MLS. For this purpose, the support needs to be enlarged and, therefore, two elements at each side of a given node are used to define its cloud. After that, the p-degree can be enhanced via extrinsic enrichment, as usually performed by PoU-based methods. This second enrichment can vary along the domain. Thus, the p-degree can be changed independently of the k-continuity.

2. MATHEMATICAL FOUNDATIONS

2.1 Galerkin's variational principle for second-order differential problems

Let the boundary-value problem be defined as: *find* $u(x) \in \mathcal{H}^1$ *such that*

$$E(x)A(x)\frac{d^2u(x)}{dx^2} + b(x) = 0 \text{ in } \Omega \qquad u = \hat{u} \text{ on } \Gamma_D \qquad t(u) = \hat{t} \text{ on } \Gamma_N \tag{1}$$

where $b(x) \in \mathcal{L}^2(\Omega, \mathbb{R}^1)$ is a distributed load, Ω is an open subset in $\mathbb{R}^1$ with boundary $\partial\Omega$. Γ_D is a Dirichlet portion of $\partial\Omega$ where $\hat{u}$ is imposed whereas Γ_N is a Neumman portion of $\partial\Omega$ where a surface external load $\hat{t}$ can be imposed. $\mathcal{L}^2(\Omega; \mathbb{R}^1)$ is the space of functions which are Lebesgue square-integrable on Ω. In Eq. (1), $E(x)$ is a distribution of Young module and $A(x)$ is a distribution of cross-section area. In linear elasticity, the stress $\sigma(x)$ is related to the strain $\varepsilon(x)$ through the linear elastic constitutive relation $\sigma(x) = E(x)\varepsilon(x)$. The strain, in turn, is related to the displacement field by the infinitesimal strain-displacement relationship $\varepsilon(x) = \frac{d}{dx}u(x)$.

The equivalent *weak form* for the Eq. (1) problem can be stated as: *find* $\tilde{u}(x) \in \mathcal{U}$ *such that*: $\mathscr{B}(\tilde{u}, \tilde{v}) = \mathscr{L}(\tilde{v}), \forall\, \tilde{v}(x) \in \mathcal{V}$. Define $\mathcal{U} \subset \mathcal{H}^1$ as the set of kinematically admissible functions, with $\mathcal{H}^1\left(\Omega; \mathbb{R}^1\right)$ being the Hilbert space containing the functions which, jointly with its first weak derivatives, are square-measurable in the Lebesgue sense. Additionally, the kinematically admissible variations $\tilde{v}$ lie in the restriction of $\mathcal{H}^1\left(\Omega; \mathbb{R}^1\right)$ with homogeneous Dirichlet boundary values, the space $\mathcal{V}$. Therefore, $\mathcal{U} := \left\{\mathcal{H}^1\left(\Omega; \mathbb{R}^1\right) : \tilde{u} = \hat{u} \text{ on } \Gamma_D\right\}$ and $\mathcal{V} := \mathcal{H}^1_D\left(\Omega; \mathbb{R}^1\right) := \left\{\tilde{v} \in \mathcal{H}^1\left(\Omega; \mathbb{R}^1\right) : \tilde{v} = 0 \text{ on } \Gamma_D\right\}$.

It is proposed a constant cross-sectional area A and Young module E, for simplicity, and it is assumed homogeneous Dirichlet boundary condition without loss of generality. The bilinear form $\mathscr{B}(\tilde{u}, \tilde{v})$, physically meaning the virtual work of the internal true stresses $\sigma(\tilde{u})$ associated with the virtual strains $\epsilon(\tilde{v})$, is a functional on $\mathcal{H}^1 \times \mathcal{H}^1 \to \mathbb{R}$, and $\mathscr{L}(\tilde{v})$ is a linear functional $\mathcal{H}^1 \to \mathbb{R}$, which represents the virtual work resulting from the external applied forces b and $\hat{t}$. They are defined as:

$$\mathscr{B}(\tilde{u}, \tilde{v}) := \int_\Omega \boldsymbol{\varepsilon}(\tilde{v})\, \sigma(\tilde{u})\, A\, dx \qquad \text{and} \qquad \mathscr{L}(\tilde{v}) := \left(\tilde{v}A\hat{t}\,\right)\big|_{\Gamma_N} + \int_\Omega \tilde{v}\, b\, dx \ . \tag{2}$$

2.2 Finite element meshes

In order to define the arbitrarily smooth weighting functions in the manner of the conventional C^k-GFEM the domain needs to be discretized with a finite element mesh. The first step is to define for each nodal coordinate x_α over the domain a set of distance functions $d_{\alpha,j}(x)$, each one associated with a neighbor x_j node. For one dimensional domains the distance functions are defined on both left and right sides of a given nodal coordinate x_α, except for nodes at the boundary of the domain where only one distance function needs to be calculated.

Figure 1 demonstrates the proposed distance functions. The usual way of defining the distance functions for the original C^k-GFEM is shown in Figure 1(a), where the cloud is composed by the two elements sharing a node. The distance functions associated with the right cloud end is pictured in dashed line whereas for the left cloud end the distance functions is displayed in continuous line. For the present modification, the clouds need to be extended, as shown in Figure 1(b), in order to accommodate the MLS procedure while intrinsically enriching the PoU with a linear basis. Then, the cloud needs to be defined by the union of element pairs at the two sides of a node. Further discussions on the requirements of the MLS method will be presented in Section 2.5.

The concept of support size for the present work will be referred to the number of elements in each side of a node. Therefore, for the weighting functions as well as for the PoU functions, compact support means that a cloud is formed by two elements. Differently, double support means that a cloud is composed by four elements.

Note that the distance functions are normalized in the sense that they measure the normalized length between a given node coordinate x_α to the respective nodes at the boundary of its cloud, with the normalization factor depending on the support size. Thus the distance functions are always unitary exactly over the nodes for which they are defined.

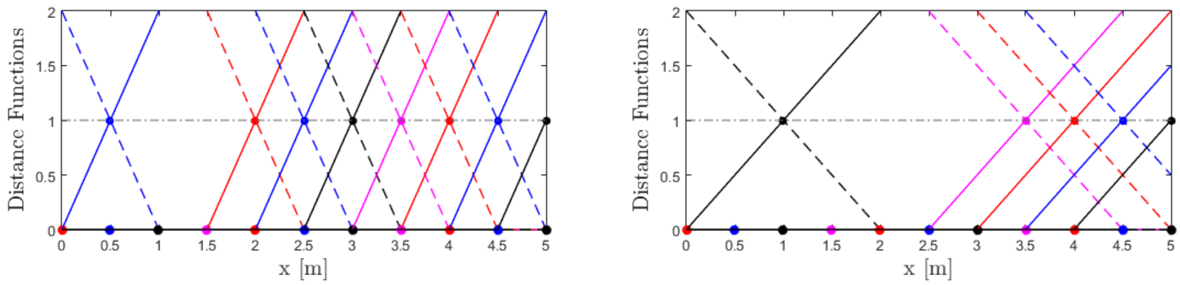

Figure 1: Distance functions $d_{\alpha,j}(x)$ defined for the nodal coordinates. For each inner node there are two distance functions related to it. (a) Compact support, where a cloud is composed by two elements. (b) Double support, where a cloud is formed by four elements.

2.3 Cloud edge functions

The cloud edge functions are defined prior to the construction of the weighting functions, as these last are defined as a product of the cloud edge functions associated to a nodal coordinate x_α. The role of cloud edge functions is to define the compact support and the arbitrary k-continuity to the weighting functions and, in the sequence, to the PoU functions. Two approaches for the construction are proposed as in Duarte *et al.* (2006) and de Barcellos *et al.* (2009): the C^∞ exponential cloud edge functions and the C^{P-1} polynomial cloud edge functions, respectively.

2.3.1 The C^{P-1} polynomial cloud edge functions

In the present work, the C^{P-1} cloud edge functions of de Barcellos *et al.* (2009) were considered. For one dimensional problems, these polynomial cloud edge functions are directly defined as monomials of degree P of the distance functions, that is:

$$\varepsilon_{\alpha,j}(x) := \begin{cases} \left(d_{\alpha,j}(x)\right)^P, & \text{if } d_{\alpha,j}(x) > 0 \\ 0, & \text{otherwise} \end{cases} \tag{3}$$

where $d_{\alpha,j}(x)$ is the j distance function associated to the nodal coordinate x_α, with $j = 1, 2$, since there are two distance functions associated to the nodal coordinate x_α. As the distance functions $d_{\alpha,j}(x)$ are strictly positive inside the cloud and unitary right at the associated node, the cloud edge functions are also positive over their respective support $\omega_{\alpha,j}$ and have an unitary value exactly over the respective nodal coordinate x_α, as seen in Figure 1. Additionally, such polynomial cloud edge functions have $P-1$ null derivatives right at the associated cloud boundary

2.3.2 The C^∞ cloud edge functions

Alternatively to the limited C^{P-1} cloud edge functions, the C^∞ cloud edge functions presented in Edwards (1996) were used to build infinitely smooth weighting functions. By defining an exponential operator for the construction of such functions it is possible to achieve $k = \infty$ continuity for the PoU resultant of them. The C^∞ cloud edge functions can be defined by:

$$\varepsilon_{\alpha,j}(x) := \begin{cases} Ae^{-\left(d_{\alpha,j}(x)/B\right)^{-\gamma}}, & \text{if } d_{\alpha,j}(x) > 0 \\ 0, & \text{otherwise} \end{cases} \tag{4}$$

where A and B are parameters defined such that the edge functions are unitary over the nodal coordinate x_α, and such that the rate of decay parameter β, defined as $\beta = \varepsilon_{\alpha,j}\left(h_{\alpha,j}/2\right)/\varepsilon_{\alpha,j}\left(h_{\alpha,j}\right)$ is enforced to be the same for the all the edge functions involved in the cloud, where $h_{\alpha,j}$ represents the cloud size, according to the support size established previously in Section 2.2 Still, the parameter γ is a positive real constant.

A proper definition of the parameters A and B can be found in Duarte *et al.* (2006) and de Barcellos *et al.* (2009). With a slight adaptation for the one dimensional domains, as the distance functions are already defined in such a way that they represent a normalized distance in the sense of the support size, the parameters A and B can be directly defined by $A = exp\big[\big((1-2^\gamma)/log_e(\beta)\big)^{-1}\big]$ and $B = \big(log_e(\beta)/(1-2^\gamma)\big)^{\frac{1}{\gamma}}$. As suggested in de Barcellos *et al.* (2009) and Duarte *et al.* (2006), $\gamma = 0.6$ and $\beta = 0.3$ are considered herein to minimize the oscillatory behavior of the PoU derivative.

2.4 Construction of the weighting functions

The weighting functions $\mathrm{W}_\alpha(x)$, as defined in Duarte *et al.* (2006) and de Barcellos *et al.* (2009), are constructed by the product of the cloud edge functions as

$$\mathrm{W}_\alpha(x) = \prod_{j=1}^{M_\alpha} \varepsilon_{\alpha,j}(x) \ . \tag{5}$$

This particular methodology for the construction of weighting functions is not unique, as splines and exponential functions are also discussed in Liu (2003). In the sense of a mesh-based method, the presented procedure is capable of recreating arbitrarily convex clouds, in higher dimensional spaces, since that n distance functions can be adapted to create a n-sided polygon.

2.5 Moving least squares approximation

The construction of the PoU via MLS method follows the reasoning: let $f(x)$ be the function for a field variable defined on the domain Ω. MLS approximation writes such field as a combination of m basis functions, that is, $\widetilde{f}(x) = \mathbf{p}(x)^T\mathbf{a}(x)$, where $\mathbf{p}(x)$ is a $m \times 1$ matrix of basis functions, and its associated coefficients $\mathbf{a}(x)$, which is a $m \times 1$ matrix.

The principle for the MLS approximation is to minimize the weighted squared residual between an exact solution and the MLS approximation field, defining weighting functions $\mathrm{W}(x, x_\alpha)$ at each x_α nodal coordinate, which are positive functions that smoothly decreases as $||x_\alpha - x||$ increases and vanishes at the boundary of its support. The weighted moment matrix $\mathbf{A}(x)$, with $m \times m$ dimension, and $\mathbf{B}(x)$, which is an $m \times 1$ matrix, are defined as:

$$\mathbf{A}(x) = \sum_{\alpha=1}^{n} \mathrm{W}(x, x_\alpha)\ \mathbf{p}(x_\alpha)\ \mathbf{p}^T(x_\alpha) \qquad\qquad \mathbf{B}(x) = \mathrm{W}(x, x_\alpha)\ \mathbf{p}(x_\alpha) \tag{6}$$

Here, a requirement of existence is set to properly define the PoU. If a vector of basis functions, which are commonly defined as complete monomials of degree up to m, $\mathbf{p}^T = \{1, x, \ldots, x^m\}$ is used, thus $n \geq m$ weighting functions are required to be non-null over any point on the domain. The reason for this is to avoid singularity of the weighted moment matrix $\mathbf{A}(x)$. Thus, if $n \geq m$ and $\mathbf{A}(x)$ is non-singular, then the MLS approximation $\widetilde{f}(x)$ and the PoU function $\phi(x)$ are defined as:

$$\begin{aligned}\widetilde{f}(x) &= \sum_{\alpha}^{n}\sum_{j}^{m} p_j(x)\Big(\mathbf{A}^{-1}(x)\,\mathbf{B}(x)\Big)_{j\alpha} f_\alpha \equiv \sum_{\alpha}^{n} \phi_\alpha(x)\ f_\alpha \\ \text{with} \quad \phi_\alpha(x) &= \sum_{j}^{m} p_j(x)\Big(\mathbf{A}^{-1}(x)\ \mathbf{B}(x)\Big)_{j\alpha} \ .\end{aligned} \tag{7}$$

Therefore, the definition $\phi_\alpha(x)$ in Eq. (7) can be employed along with a properly built $\mathrm{W}(x, x_\alpha) = \mathrm{W}_\alpha(x)$, using different types of edge functions as in the original C^k-GFEM. While constructing the PoU with $\mathbf{p} = \{1, x\}$, function's support size should be adapted to guarantee the requirement hereby discussed.

2.6 Extrinsic enrichment of Partitions of Unity

The PoU functions $\phi_\alpha(x)$ constructed via MLS method can be extrinsically enriched by multiplying them to a set of enrichment functions $\{L_{i\alpha}\}_{i=1}^{p}$, where p is the number of enrichment functions associated with the node x_α. For the present work, enrichment is done by defining a set of complete monomials for each node, which is defined as $\mathcal{P}_p(\omega_\alpha) \subset \mathcal{X}_\alpha^p(\omega_\alpha)$, with $\mathcal{P}_p$ standing for the space of polynomials of degree up to p on the cloud ω_α. Thus, the local approximation subspaces can be denoted as $\mathcal{X}_\alpha(\omega_\alpha) = span\{L_{i\alpha}\}_{i\in\mathcal{I}(\alpha)}$, as generally performed in GFEM framework.

The set of enrichment functions are defined as $L_{i\alpha} = [1, \overline{x}, \overline{x}^2, \ldots, \overline{x}^p]$, where $\overline{x}$ is an intrinsic coordinate defined from each node x_α as $\overline{x} = (x - x_\alpha)/l_e$. The scaling factor l_e, which was here taken as the finite element size, is recommended in Mendonça *et al.* (2013) to reduce round-off errors.

In this way, the discretized version of Galerkin's variational principle can be solved using the Galerkin expansion:

$$\widetilde{u}(x) = \sum_{\alpha=1}^{N} \phi_\alpha\,(x) \left\{ c_\alpha + \sum_{i=2}^{q_\alpha} L_{i\alpha}\,(\overline{x})\;\, d_{i\alpha} \right\} \tag{8}$$

where $d_{i\alpha}$ is a generalized nodal coefficient associated with each enrichment function $L_{i\alpha}$ of the node x_α, and q_α is the number of enrichment functions associated to it. Finally, c_α is the coefficient associated to the PoU function $\phi_\alpha(x)$.

2.7 Boundary conditions and the intrinsically enriched PoU

The MLS methodology for the construction of PoU is known to produce functions that does not possesses the Kronecker delta property, as stated in Liu (2003) and discussed in Lancaster and Salkauskas (1981). Alternative methodologies to couple FEM shape functions and MLS shape functions have been presented in order to enforce boundary conditions similarly to the conventional FEM (Belytschko and Krongauz, 1996; Belytschko *et al.*, 1989; Duarte *et al.*, 2005; Hegen, 1996; Huerta and Méndez, 2000; Belytschko *et al.*, 1995).

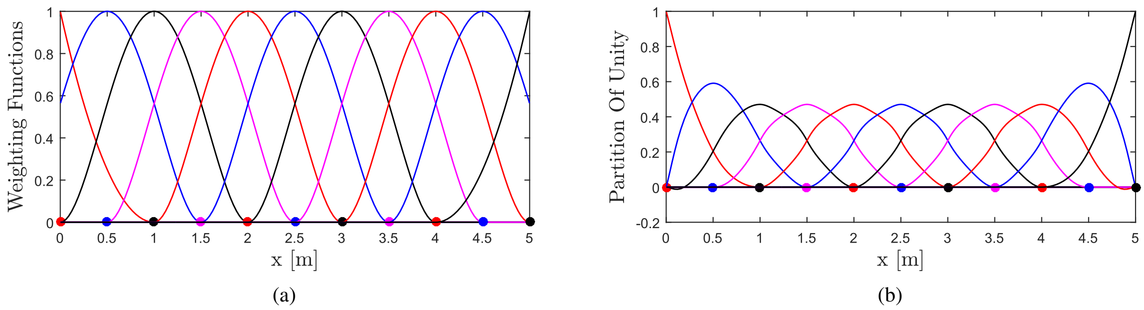

Figure 2: Intrinsically enriched MLS PoU on the *conventional* cloud edge functions approach: double support and intrinsic enrichment $p = 1$ for the cloud edge degree $P = 2$. (a) Weighting functions. (b) PoU.

For one dimensional problems, however, while constructing the PoU with double support over the entire domain and attributing an intrinsic $p = 1$ enrichment, the PoU associated to the nodes exactly at the domain boundary naturally recovers the Kronecker delta property, as exactly $n = m$ clouds are defined over such nodes. A graphical representation of weighting functions with double support, as well as the associated PoU, can be seen in Fig. (2), where the PoU has the unitary value at the boundary at $x = 0$ and $x = 5$.

For the proposition presented in Figure (2.a), the PoU naturally recovers the Kronecker delta property as the $n \geq m$ (two weighting functions or more, for intrinsic enrichment with $p = 1$) condition established before is exactly satisfied by imposing double support for the cloud edge functions. That is, exactly two weighting functions are defined over the coordinates at the boundary of the domain, where boundary conditions are here imposed.

Still, for the present analysis, when no intrinsic enrichment is attributed to the PoU the weighting functions will always be constructed with compact support to preserve the naturally inherited Kronecker delta property of the PoU. A graphical representation can be seen in Figure 3.

3. NUMERICAL RESULTS

For the performance assessment of the presented method two linear elastic one dimensional problems are proposed. Firstly, a smooth polynomial distributed load is considered to study the capability of the method to represent polynomial regular solutions. As a second problem, a smooth force field with a high gradient in a small subdomain is presented.

Uniform mesh discretizations with $10, 20, 40$ and 80 elements were considered. The quality of the approximations is measured by the relative error in terms of the $\mathcal{L}^2(\Omega)$ norm for displacement fields, as well as the relative error in terms of the $\mathcal{L}^2(\Omega)$ norm for strain fields, and the stiffness matrix condition number and its respective bandwidth are considered here as an evaluation of the computational costs.

Double support was used to make feasible the construction of PoU functions via MLS method considering intrinsic $p = 1$ enrichment, while employing a vector of basis functions $\mathbf{p}^T(x) = \{1, x - 10\}$. Different types of cloud edge functions. For instance, besides the conventional exponential edge functions, which assign C^∞ continuity for the weighting functions, lower regularity orders were obtained with monomials of degree P. Edge degrees of $P = 2, 3$ and 4 where

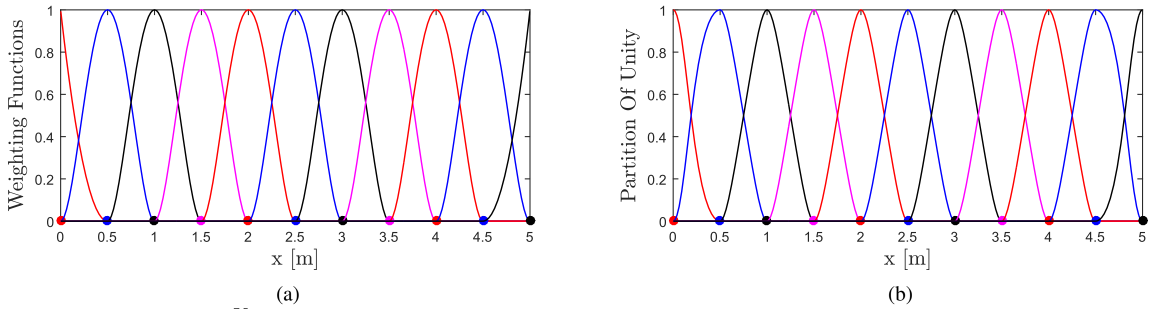

Figure 3: *Conventional* C^K-GFEM: compact support with no intrinsic enrichment, for the cloud edge degree $P = 2$. (a) Weighting functions. (b) PoU.

considered, and cloud edge functions with C^1, C^2 and C^3 continuity were obtained, respectively, comprehending the C^{P-1} continuous edge functions presented in de Barcellos *et al.* (2009).

The evaluation of the experimental convergence rates was achieved by curve fitting of the data considering an expression in the form $\|e\|_{\mathcal{L}^2} = Ch^{\beta_h}$, where C is a problem dependent constant, h is the element length and β_h is the convergence rate. For the first problem, the fitting procedure was done after all the relative $\mathcal{L}^2$ norms of error on displacement and strain were obtained, while fitting all norms at once.

For the second problem the convergence rates were evaluated by fitting $\|e\|_{\mathcal{L}^2} = Ch^{\beta_h}$ at two consecutive levels of degrees of freedom, as the relative error norm curves did not exhibit a linear aspect as in the first problem.

Still, the comparison is done according to the polynomial attribute of both resulting approximations. For instance, to compare the $p = 1$ intrinsically enriched PoU, the conventional C^k-GFEM PoU was extrinsically enriched with $p = 1$. Additionally, to compare a $p = 1$ intrinsically, and further $p = 1$ extrinsically enriched PoU, the conventional C^k-GFEM PoU was extrinsically enriched with $p = 2$.

The intrinsically enriched C^k-GFEM will be referred as the MLS approximation, P will be referred to the cloud edge function degree $(2, 3, 4$ and $\infty)$, and the convergence rates for the displacement error norm $\mathcal{L}^2(u_x)$ and for strain error norm $\mathcal{L}^2(\varepsilon_x)$ will be referred as $\beta_h(u_x)$ and $\beta_h(\varepsilon_x)$, respectively. The MLS PoU will be constructed along with the consideration of double support, in order to accommodate the intrinsic enrichment, while the C^k-GFEM PoU will be strictly constructed with compact support (Figure 3).

For the integration procedures on both presented problems, 25 Gaussian quadrature points were found to be adequate within a given level of error. The amount of required points were defined after a set of experimental tests on the worst condition were made, that is, a convergence analysis of the terms of the stiffness matrix, as well as the terms of the external force vector, on the 80 elements discretization for both cloud edge degrees $P = 4$ and $P = \infty$ while intrinsically enriching the PoU.

3.1 Smooth polynomial distributed load

As a first numerical evaluation of the method, the linear elastic problem of a rod with constant cross-section area $A = 1$ square meters and length $L = 5$ meters, such that $\Omega = [0; 5 \text{ meters}]$, subjected to an external distributed force $b(x) = 1 - 2x + \frac{3}{2}x^2$ Newton / meter. The Young module $E = 10$ Pascal is used. The prescribed boundary conditions are: for displacement, $u(x = 0) = 0$ meter (restrained end at $x = 0$ meters), and for stress, $\sigma(x = 5) = 0$ Pascal (free end at $x = 5$ meters).

Firstly, the linear basis was attributed to the MLS PoU with no extrinsic enrichment, and the extrinsic enrichment $p = 1$ was attributed to the C^k-GFEM PoU, thus sharing the same polynomial degree. For the presented considerations with respect to the support size and intrinsic enrichment, both of the PoU's share the same matrix bandwidth. Figure 4 shows the respective experimental data.

The intrinsically enriched PoU (presented as the MLS approximation) manifested a superior performance than the conventional C^k-GFEM in terms of relative norms of error for both displacement and strain, and a notable reduction of the stiffness matrix condition number was found for any of the edge functions P degrees considered.

Note that in terms of experimental convergence rates for displacement and strain, the MLS PoU was capable of overcoming the convergence rates even for the conventional piece-wise linear FEM approximation, except when using edge functions with $P = 2$ degree, which renders C^1 approximations for the MLS PoU as well as the C^k-GFEM. Still, the approximation reached by the MLS PoU is notably better than the conventional C^k-GFEM and FEM.

As the extrinsic enrichment of the C^k-GFEM approach is increased to $p = 2$ and the MLS PoU receives the extrinsic enrichment of $p = 1$, that is, presenting an equivalent polynomial basis of degree $p = 2$ (extrinsic + intrinsic degree) for both PoU's, the MLS PoU does not show considerably improvement with relation to the conventional C^k-GFEM, even

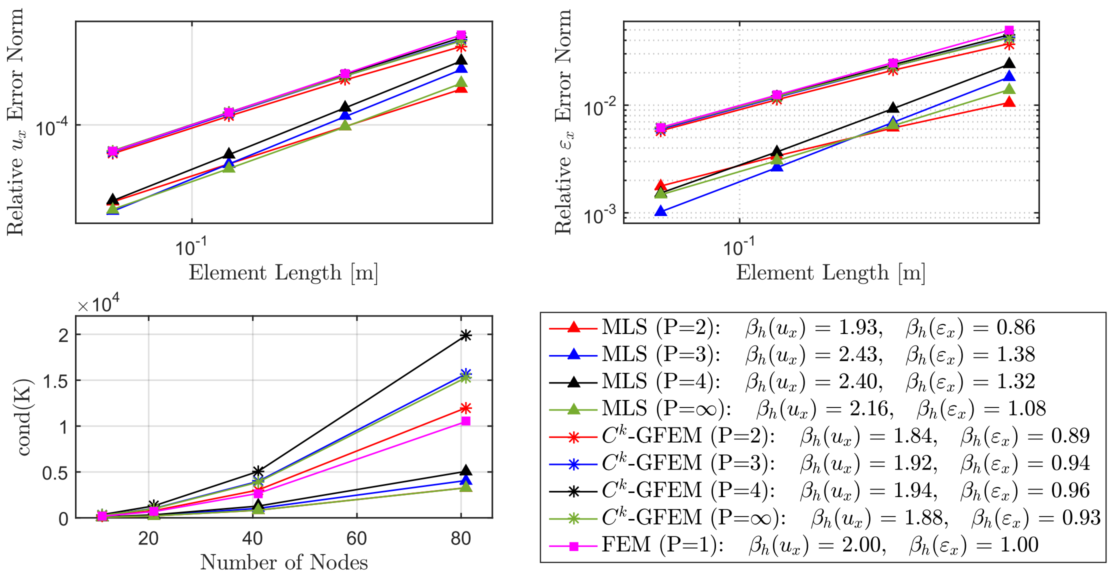

Figure 4: Results for both MLS (intrinsic $p = 1$, extrinsic $p = 0$) and C^k-GFEM (extrinsic $p = 1$) PoU. Upper left: evolution of the relative displacement error norm. Upper right: evolution of the relative strain error norm. Bottom left: evolution of the stiffness matrix condition number.

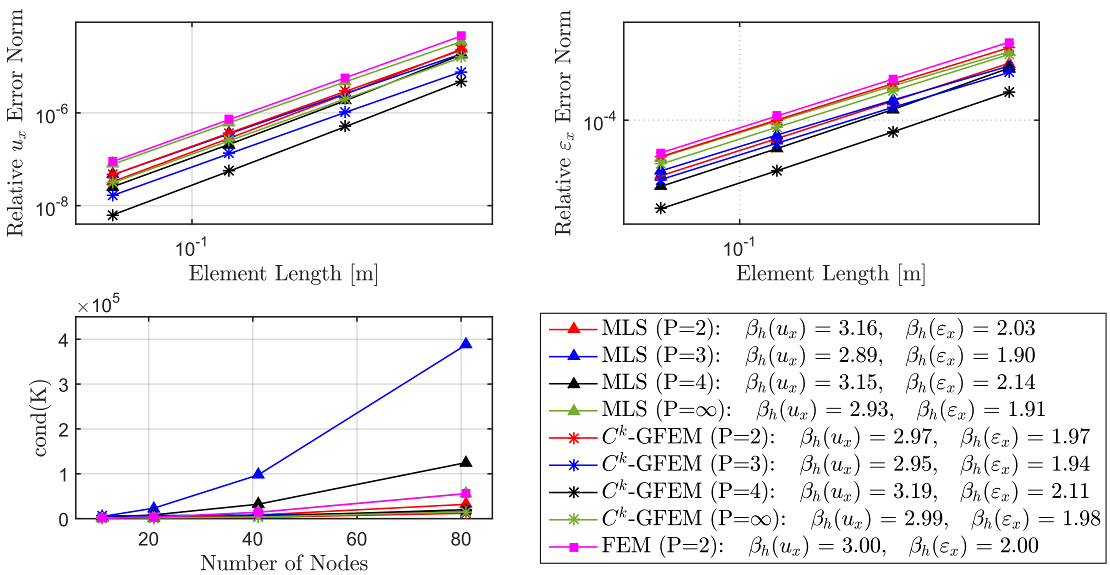

Figure 5: Results for both MLS (intrinsic $p = 1$, extrinsic $p = 1$) and C^k-GFEM (extrinsic $p = 2$) PoU. Upper left: evolution of the relative displacement error norm. Upper right: evolution of the relative strain error norm. Bottom left: evolution of the stiffness matrix condition number.

though MLS with $P = 2$ and $P = 4$ and C^k-GFEM with $P = 4$ still slightly outperform the conventional FEM. The respective data for the proposed PoU can be seen in Figure 5.

The enriched methodologies only exceed the performance of the conventional FEM with quadratic shape functions, in terms of experimental convergence rates, in case of MLS ($P = 2$ and $P = 4$) and C^k-GFEM ($P = 4$).

Even while presenting approximations at the same level as the conventional C^k-GFEM, the MLS PoU stiffness matrix condition number is considerably higher than its counterpart, while presenting little gain or losses on the experimental convergence rates and a higher matrix bandwidth (15 for the MLS, 11 for the C^k-GFEM).

From these results, considering the superior complexity to build the intrinsically enriched C^k-GFEM PoU and the numerical evaluations, the conventional C^k-GFEM presents a computational advantaged over the MLS PoU in terms of implementation aspects.

3.2 Smooth high gradient distributed load

The following problem was presented in Rachowicz *et al.* (1989). An analytically smooth, with high gradient, external distributed force field $b(x)$ is applied to a rod with constant cross sectional area $A = 1$ square meters and constant Young module $E = 1$ Pascal. The force field is given by:

$$b(x) = 2\alpha \left[\frac{1}{1 + \alpha^2 (x - x_0)^2} + \frac{\alpha^2 (x - x_0)(1 - x)}{\left[1 + \alpha^2 (x - x_0)^2\right]^2} \right] \tag{9}$$

where α is a parameter that controls the magnitude of the gradient at the specified coordinate x_0.

3.2.1 High gradient at $x_0 = 0$ meters and $\alpha = 50$

As a first approach for the proposed problem, both MLS PoU (intrinsic $p = 1$, extrinsic $p = 0$) and the C^k-GFEM PoU (extrinsic $p = 1$) PoU were used. The respective experimental data is presented in Table 1. For this problem the cloud edge degrees $P = 2, 3, 4$ and ∞ are still attributed. For both displacement and strain field approximations the C^k-GFEM, in most cases, generates a better approximation in terms of relative error norms than the MLS approaches when the discretization with 10 elements (11 nodes) is proposed.

Most of the experimental convergence rates for both approaches of the MLS PoU are found to be as double of the value of the ones obtained from the C^k-GFEM approximation for the set of cloud edge functions and meshes used, even for strain norms. The MLS PoU produced a greater stiffness matrix condition number than the C^k-GFEM, still generating better approximations as the h-refinement is applied to the mesh and greater experimental convergence rates.

Table 1: Approximation for the smooth high gradient load at $x_0 = 0$ for the MLS PoU (intrinsic $p = 1$, extrinsic $p = 0$) and the C^k-GFEM (extrinsic $p = 1$). The values in bold exceed the respective obtained for the conventional C^k-GFEM

		MLS					C^k-GFEM				
Edge	Nodes	$\mathcal{L}^2(u_x)$	$\beta_h(u_x)$	cond(K)	$\mathcal{L}^2(\varepsilon_x)$	$\beta_h(\varepsilon_x)$	$\mathcal{L}^2(u_x)$	$\beta_h(u_x)$	cond(K)	$\mathcal{L}^2(\varepsilon_x)$	$\beta_h(\varepsilon_x)$
2	11	7.29e−2	–	2.08e+1	4.50e−1	–	4.21e−2	–	5.35e+1	2.81e−1	–
	21	2.06e−2	1.82	3.58e+1	2.00e−1	1.17	1.42e−2	1.57	1.88e+2	1.71e−1	0.71
	41	3.26e−3	**2.66**	1.27e+2	5.92e−2	**1.76**	6.39e−3	1.15	7.41e+2	1.38e−1	0.31
	81	5.03e−4	**2.70**	5.06e+2	2.80e−2	**1.08**	2.54e−3	1.33	2.96e+3	9.78e−2	0.50
3	11	1.10e−1	–	1.14e+1	6.34e−1	–	5.72e−2	–	6.65e+1	3.50e−1	–
	21	3.64e−2	1.59	4.40e+1	3.78e−1	0.75	2.14e−2	1.30	2.46e+2	2.33e−1	0.59
	41	6.96e−3	**2.39**	1.75e+2	1.37e−1	**1.46**	9.82e−3	1.13	9.72e+2	1.85e−1	0.33
	81	7.72e−4	**3.17**	6.97e+2	3.17e−2	**2.11**	3.44e−3	1.51	3.88e+3	1.19e−1	0.64
4	11	1.32e−1	–	1.52e+1	6.96e−1	–	5.58e−2	–	8.39e+1	3.85e−1	–
	21	4.64e−2	1.51	5.93e+1	4.50e−1	0.63	2.50e−2	1.16	3.13e+2	2.60e−1	0.56
	41	9.73e−3	**2.25**	2.36e+2	1.87e−1	**1.27**	1.17e−2	1.10	1.23e+3	2.07e−1	0.33
	81	1.20e−3	3.02	9.42e+2	4.91e−2	**1.93**	3.88e−3	1.59	4.92e+3	1.28e−1	0.69
∞	11	7.82e−2	–	1.35e+1	5.14e−1	–	5.90e−2	–	6.49e+1	3.80e−1	–
	21	2.05e−2	1.94	3.79e+1	2.40e−1	1.10	2.09e−2	1.50	2.41e+2	2.37e−1	0.68
	41	3.22e−3	**2.67**	1.33e+2	7.44e−2	**1.69**	8.66e−3	1.27	9.50e+2	1.72e−1	0.46
	81	7.19e−4	2.16	5.32e+2	3.81e−2	0.97	3.19e−3	1.44	3.79e+3	1.13e−1	0.60
Bandwidth		7					7				

Table 1: (*Continuation*) Approximation for the smooth high gradient load at $x_0 = 0$ for the conventional Lagrange linear shape functions

	C^0-FEM (Linear Lagrange PoU)				
Nodes	$\mathcal{L}^2(u_x)$	$\beta_h(u_x)$	cond(K)	$\mathcal{L}^2(\varepsilon_x)$	$\beta_h(\varepsilon_x)$
11	1.61e−1	–	3.99e+1	7.45e−1	–
21	6.32e−2	1.35	1.61e+2	5.29e−1	0.49
41	1.72e−2	1.88	6.48e+2	2.82e−1	0.91
81	4.01e−3	2.10	2.59e+3	1.32e−1	1.09
Bandwidth	3				

The experimental data for the present problem for both MLS PoU (intrinsic $p = 1$, extrinsic $p = 1$) and the C^k-GFEM (extrinsic $p = 2$) approximations can be found in Table 2. Once more, the MLS PoU provides a wider bandwidth as the extended support is needed to attribute the intrinsic enrichment. While generating a better bandwidth, the C^k-GFEM still generates a greater conditioning number for the stiffness matrix, presenting small increments as the h-refinement occurs.

Note that for any of the edge function degrees considered here the C^k-GFEM presented a better approximation in terms of relative error norms for all mesh discretizations, both on displacement and strain fields. Yet, the data propose that the extrinsically enriched C^k-GFEM, even while generating convergence rates not greater than the MLS PoU, is still capable of generating better conditioning number for the stiffness matrix and yet a better approximation for the fields.

Table 2: Approximation for the smooth high gradient load at $x_0 = 0$ for the MLS PoU (intrinsic $p = 1$, extrinsic $p = 1$) and the C^k-GFEM (extrinsic $p = 2$). The values in bold exceed the respective obtained for the conventional C^k-GFEM.

		MLS					C^k-GFEM				
Edge	Nodes	$\mathcal{L}^2(u_x)$	$\beta_h(u_x)$	cond(K)	$\mathcal{L}^2(\varepsilon_x)$	$\beta_h(\varepsilon_x)$	$\mathcal{L}^2(u_x)$	$\beta_h(u_x)$	cond(K)	$\mathcal{L}^2(\varepsilon_x)$	$\beta_h(\varepsilon_x)$
2	11	5.15e−2	–	8.87e+2	2.99e−1	–	8.26e−3	–	2.21e+3	9.88e−2	–
	21	8.03e−3	**2.68**	1.96e+3	8.73e−2	**1.78**	1.61e−3	2.36	2.24e+3	3.90e−2	1.34
	41	1.09e−3	**2.89**	6.83e+3	3.06e−2	**1.51**	3.51e−4	2.20	2.25e+3	1.82e−2	1.10
	81	3.24e−4	1.74	2.63e+4	1.50e−2	1.03	8.36e−5	2.07	2.96e+3	7.33e−3	1.31
3	11	2.78e−2	–	3.79e+3	2.02e−1	–	2.64e−3	–	6.07e+3	4.72e−2	–
	21	3.12e−3	**3.16**	1.90e+4	4.92e−2	**2.04**	6.12e−4	2.11	6.95e+3	2.52e−2	0.90
	41	3.66e−4	**3.09**	7.90e+4	1.32e−2	**1.90**	2.06e−4	1.57	7.85e+3	1.29e−2	0.97
	81	9.71e−5	1.91	3.15e+5	5.76e−3	1.19	2.71e−5	2.93	8.32e+3	3.29e−3	1.97
4	11	2.38e−2	–	1.97e+3	2.36e−1	–	1.78e−3	–	1.55e+3	3.35e−2	–
	21	2.72e−3	**3.13**	6.97e+3	5.07e−2	**2.22**	1.30e−3	0.45	1.57e+3	3.64e−2	−0.12
	41	3.53e−4	**2.94**	2.64e+4	1.78e−2	**1.51**	4.10e−4	1.66	1.58e+3	1.86e−2	0.97
	81	8.14e−5	2.12	1.03e+5	7.20e−3	1.30	7.65e−6	5.74	4.93e+3	9.64e−4	4.27
∞	11	4.86e−2	–	7.74e+2	2.85e−1	–	9.46e−3	–	1.91e+3	1.27e−1	–
	21	1.00e−2	2.28	3.16e+3	1.07e−1	1.42	1.64e−3	2.53	1.94e+3	4.42e−2	1.53
	41	6.69e−4	**3.90**	1.25e+4	2.06e−2	**2.37**	2.84e−4	2.53	1.95e+3	1.73e−2	1.35
	81	3.52e−4	0.93	4.91e+4	1.59e−2	0.37	7.17e−5	1.98	3.79e+3	7.31e−3	1.24
Bandwidth		15					11				

Table 2: (*Continuation*) Approximation for the smooth high gradient load at $x_0 = 0$ for the the conventional Lagrange linear shape functions (extrinsic $p = 1$).

	C^0-GFEM (Linear Lagrange PoU, extrinsic $p = 1$)				
Nodes	$\mathcal{L}^2(u_x)$	$\beta_h(u_x)$	cond(K)	$\mathcal{L}^2(\varepsilon_x)$	$\beta_h(\varepsilon_x)$
11	4.15e−2	–	1.44e+2	3.60e−1	–
21	7.60e−3	2.45	5.34e+2	1.26e−1	1.52
41	6.45e−4	3.56	2.04e+3	2.63e−2	2.26
81	2.34e−4	1.46	7.98e+3	1.59e−2	0.73
Bandwidth	7				

4. CONCLUSIONS AND REMARKS

The intrinsically enriched C^k-GFEM PoU via MLS method with a linear polynomial basis presented a greater performance than the conventional C^k-GFEM extrinsically enriched with the same polynomial basis for the proposed problems. Visible advantage of the MLS PoU was found for the conditions where no extrinsic enrichment was attributed to the MLS PoU, and minor advantages were found with the extrinsic enrichment for the same PoU's.

For the proposed considerations for the construction of the PoU, when extrinsic enrichment is attributed to the MLS PoU the intrinsically enriched Partitions presented wider stiffness matrix bandwidth and higher conditioning numbers, still presenting however less DOF's than the conventional C^k-GFEM.

Note also that while extending the function's support size in order to accommodate the intrinsic enrichment, each node is capable of affecting a larger portion of the respective problem domain as more interactions between the Partition of Unity functions and the extrinsic enrichment functions will occur. This can be comprehended as the widening of the stiffness matrix bandwidth. Increasing the extrinsic enrichment for the MLS PoU widens the stiffness matrix at a greater rate than the C^k-GFEM. Still, lesser degrees of freedom are found for the MLS PoU considering an equivalent polynomial basis (extrinsic + intrinsic enrichment).

5. REFERENCES

Belytschko, T., Chang, H.S. and Lu, Y.Y., 1989. "A variationally coupled finite element-boundary element method". *Computer & Structures*, Vol. 33, No. 1, pp. 17–20.

Belytschko, T. and Krongauz, Y., 1996. "A coupled finite element-element-free galerkin method". *Computer Methods in Applied Mechanics and Engineering*, , No. 131, pp. 13–145.

Belytschko, T., Lu, Y.Y. and Gu, L., 1994. "Element-free galerkin method". *International Journal for Numerical Methods in Engineering*, Vol. 37, pp. 229–256.

Belytschko, T., Moës, N., Usui, S. and Parimi, C., 2001. "Arbitrary discontinuities in finite elements". *International Journal for Numerical Methods in Engineering*, Vol. 50, pp. 993–1013.

Belytschko, T., Organ, D. and Krongauz, Y., 1995. "A coupled finite element-element-free galerkin method". *Computational Mechanics*, , No. 17, pp. 186–195.

Cottrell, J.A., Hughes, T.J.R. and Reali, A., 2007. "Studies of refinement and continuity in isogeometric structural analysis". *Computer Methods in Applied Mechanics and Engineering*, Vol. 196, No. 41-44, pp. 4160–4183.

de Barcellos, C.S., Mendonça, P.T.R. and Duarte, C.A., 2009. "A C^k continuous generalized finite element formulations applied to laminated kirchhoff plate model". *Computational Mechanics*, Vol. 44, pp. 377–393.

Duarte, C.A., Babuška, I. and Oden, J.T., 2000. "Generalized finite element method for three-dimensional structural mechanics problems". *Computers and Structures*, Vol. 77, pp. 215–232.

Duarte, C.A., Kim, D.J. and Quaresma, D.M., 2006. "Arbitrarily smooth generalized finite element approximations". *Computer Methods in Applied Mechanics and Engineering*, Vol. 196, pp. 33–56.

Duarte, C.A., Migliano, D.Q. and Becker, E.B., 2005. "A technique to combine meshfree- and finite element-based partition of unity approximations". Structural Research Series 638, University of Illinois at Urbana-Champaign.

Duarte, C.A. and Oden, J.T., 1996. "An $h-p$ adaptive method using clouds". *Computer Methods in Applied Mechanics and Engineering*, Vol. 139, No. 1-4, pp. 237–262.

Edwards, H.C., 1996. "c^∞ finite element basis functions". Report 96-45, University of Texas at Austin.

Hegen, D., 1996. "Element-free galerkin methods in combination with finite element approaches". *Computer Methods in Applied Mechanics and Engineering*, , No. 135, pp. 143–166.

Huerta, A. and Méndez, S.F., 2000. "Enrichment and coupling of the finite element and meshless methods". *International Journal For Numerical Methods In Engineering*, , No. 48, pp. 1615–1636.

Lancaster, P. and Salkauskas, K., 1981. "Surfaces generated by moving least squares methods". *Mathematics of Computation*, Vol. 37, No. 155, pp. 141–158.

Liu, G.R., Dai, K.Y. and Nguyen, T.T., 2007. "A smoothed finite element method for mechanics problems". *Computational Mechanics*, Vol. 39, No. 6, pp. 859–877.

Liu, G., 2003. *Meshfree methods: moving beyond the Finite Element Method*. CRC Press.

Malagù, M., Benvenuti, E., Duarte, C.A. and Simone, A., 2014. "One-dimensional nonlocal and gradient elasticity: assessment of high order approximation schemes". *Computer Methods in Applied Mechanics and Engineering*, Vol. 275, pp. 138–158.

Mendonça, P.T.R., de Barcellos, C.S. and Torres, D.A.F., 2013. "Robust c^k/c^0 generalized fem approximations for higher-order conformity requirements: application to reddy's hsdt model for anisotropic laminated plates". *Composite Structures*, Vol. 96, pp. 332–345.

Moës, N., Dolbow, J. and Belytschko, T., 1999. "A finite element method for crack growth without remeshing". *International Journal for Numerical Methods in Engineering*, Vol. 46, pp. 131–150.

Rachowicz, W., Oden, J.T. and Demkowicz, L., 1989. "Toward a universal $h-p$ adaptative finite element strategy part 3. design of $h-p$ meshes". *Computer Methods in Applied Mechanics and Engineering*, , No. 77, pp. 181–212.

Schweitzer, M.A., 2008. "Meshfree and generalized finite element methods". (Habilitation thesis), R. F. -W. Universität Bonn.

Surana, K.S., Petti, S.R., Ahmadi, A.R. and Reddy, J.N., 2001. "On p-version hierarchical interpolation functions for higher-order continuity finite element models". *International Journal of Computational Engineering Science*, Vol. 2, No. 4, pp. 653–673.

Torres, D.A.F., de Barcellos, C.S. and Mendonça, P.T.R., 2015. "Effects of the smoothness of partitions of unity on the quality of representation of singular enrichments for gfem/xfem stress approximations around brittle cracks". *Computer Methods in Applied Mechanics and Engineering*, Vol. 283, pp. 243–279.

6. RESPONSIBILITY NOTICE

The authors are the only responsible for the printed material included in this paper.